The tidal bore in the Sittaung River

A sensitivity analyse of the propagation

M.P. de Ridder

Technische Universiteit Delft

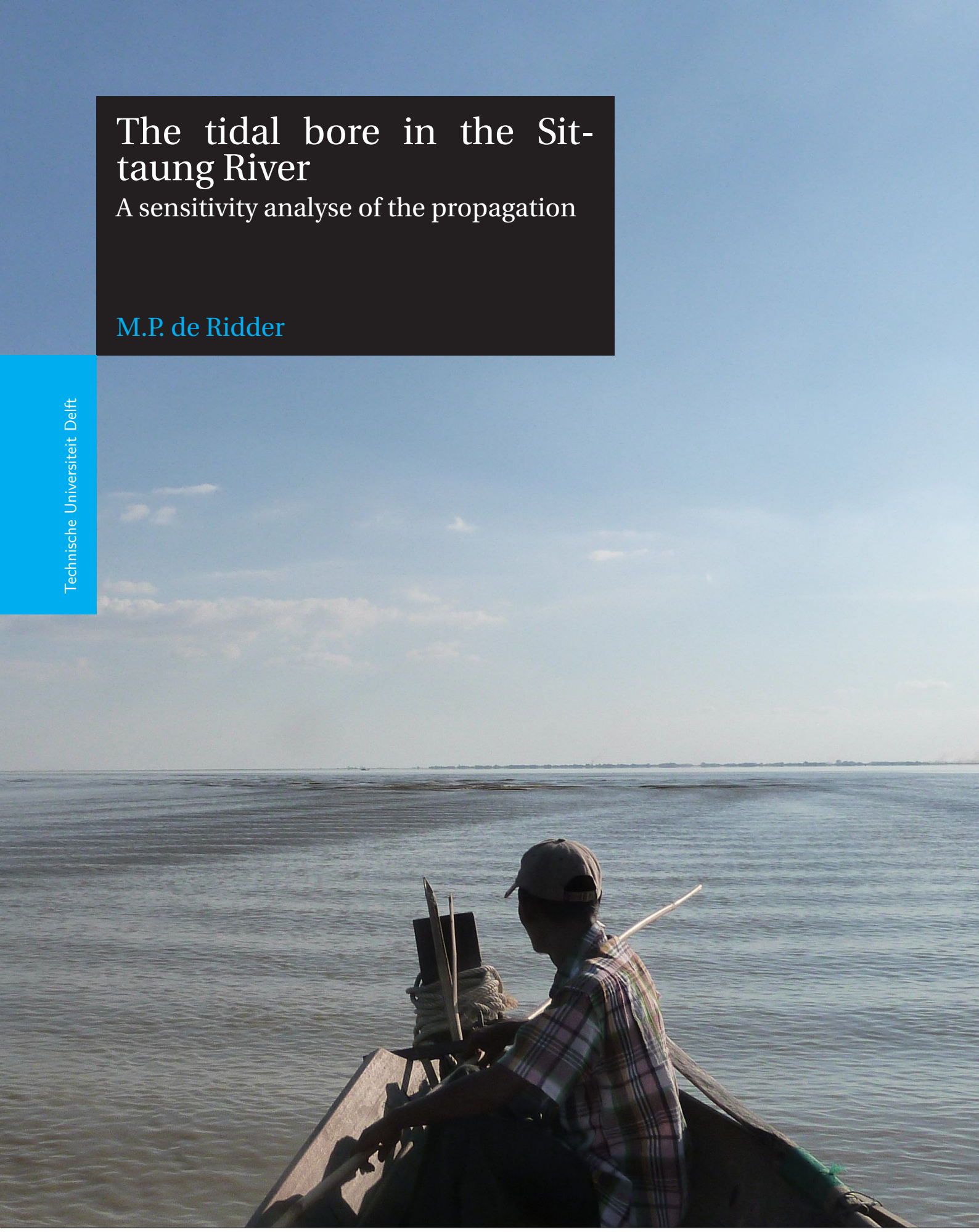

TU Delft Delft University of Technology

Challenge the future

THE TIDAL BORE IN THE SITTAUNG RIVER

A SENSITIVITY ANALYSE OF THE PROPAGATION

by

M.P. de Ridder

Additional thesis
Master Hydraulic Engineering and Water Resource Management

at the Delft University of Technology.

Student number: 4230965
Supervisor: Prof. dr. ir. Z.B. Wang
Dr. ir. M.M. Rutten

TU Delft Delft University of Technology

PREFACE

This thesis is part of my master Hydraulic Engineering and Water Resource Management at the TU Delft and NUS Singapore. The research is done in collaboration with the Myanmar Maritime University.

I would like to thank everyone from the Myanmar Maritime University who helped me during my stay in Myanmar. Especially Khin Kyi Cin Linn for collaborating in this study. Without your help, it was not possible to do this study. I also thank my supervisors, Zheng Bing Wang and Martine Rutten, for their feedback.

M.P. de Ridder
Delft, January 2017

ABSTRACT

A 2D numerical model is set-up for the tidal bore in the Sittaung River. This model is used to analyse the effect of the bottom friction, bathymetry, tidal range and river discharge on the propagation of the tidal bore. To obtain information about the tidal bore the Sittaung River is visited two times. During the second visit, depth measurements were carried out. It became clear that the tidal bore occurs only a few days after full and new moon at the village Kyaik Ka Thar. The tidal bore is also observed near Kyaik Ka Thar as an undular bore with a height of ± 0.3 m. Downstream in the estuary the tidal bore is larger and occurs 5 till 7 days after full and new moon.

A numerical model is set-up for the region from Madauk till the Gulf of Marteban. The bathymetry is based on various datasets. Only a few cross-sectional profiles were available for the upper part of the model. The SRTM map was used to determine the bottom slope of the river, whereas the cross-sections were used to determine the cross-sectional profile. From the depth measurements the initial depth for the bottom slope was obtained. The Navioncs webapp is used for the lower part of the domain (Gulf of Martaban). Both parts of the bathymetry were connected by using linear interpolation. From the Landat pictures the locations of the intertidal areas were obtained. As an upstream boundary a river discharge is set. A tidal signal is used as the downstream boundary. This downstream signal consists of two components: a daily double high water signal (D2) and a daily quarter high water signal (D4). The calibration is based on the propagation of the tidal bore. When the water level changes are larger than 0.2 m within 2.5 minute it is assumed that the tidal bore has propagate through a grid cell. On this way, the model results could be calibrated with data obtained from the field. For verification the relation between the cross-sectional area and the tidal prism was checked. For the sensitivity analyse the bottom friction, tidal range, bathymetry and river discharge were varied in various simulations. From these results can be concluded that the river discharge has no influence on the tidal bore, whereas the other parameters has a significant effect on the tidal bore. This implies that damming the Sittaung River, resulting in a change of the discharge, will not affect the tidal bore. Thus, changes of the propagation are only caused by the geometry and bathymetry of the estuary. Secondly the variety of the tidal bore is only caused by the tidal range, because this is the only parameter which change throughout the year. At least the effect of the tidal bore on the erosion is checked, but it is very difficult to relate the tidal bore to the erosion due to the lack of data. Upstream in the estuary the tidal bore is a small undular bore, which will not cause must erosion. Downstream of the estuary the tidal bore is larger and could have much more effect on the erosion.

CONTENTS

1

INTRODUCTION

This study is about the tidal bore in the Sittaung River. The Sittaung River is located in Myanmar and flows into the Gulf of Martaban. At the mouth of the River the tidal wave is deformed in such a way that the tidal wave propagates as a front (tidal bore) into the river. This front makes it for example impossible for ships to sail at the mouth of the Sittaung River. Therefore, the lower course is linked to the Bago River to bypass the tidal bore.

Two types of tidal bore can be classified based on their Froude number [1]. A breaking bore occurs when the Froude number is larger than 1.7-1.8, while an undular bore occurs for smaller Froude numbers. An undular bore is a larger wave followed by a train of secondary waves, while the breaking bore is more like a wall of water. The circumstances for the occurrence of a tidal bore are very specific. Therefore, not many estuaries have a tidal bore [2]. The most important factors for the formation of a tidal bore are the tidal range, freshwater discharge, estuary geometry and the channel bathymetry [3]. It is known that tidal bores appear in estuaries with a large tidal range and a funnel shape [4]. A tidal wave will deform when it propagates into shallow water. In shallow water the wave celerity varies over the tidal wave, causing tidal asymmetry. The speed of the crest is higher, $c = \sqrt{g(h_0 + a)}$, than the speed of the through, $c = \sqrt{g(h_0 - a)}$. This results in a faster rising period than a falling period. If this difference is very large, the rising period will become very small. This will result in a steep front which propagate into the estuary. Due to the funnel shape of an estuary the tidal amplitude will amplify. This can be seen from a simple energy balance. The energy balance for waves (assuming no friction) is given by,

$$Encb_s = constant \rightarrow \hat{\eta}\sqrt{gh}b_s \tag{1.1}$$

Where E is the energy, nc is the group velocity and b_s the width. From this balance the following relation can be derived,

$$\frac{\hat{\eta_2}}{\hat{\eta_1}} = \frac{h_1}{h_2}^{1/4} \frac{b_{s1}}{h_{s2}}^{1/2} \tag{1.2}$$

Where η is the amplitude, h the water depth and b_s the width at two locations along the channel axis (1 and 2). From this relation, it can be deduced that width reduction has a larger effect than depth reduction on the amplitude [5]. This shows why the funnel shape is an important factor for the formation of a tidal bore. Besides the shallow-water effect, the bottom friction causes the tidal wave to deform. During low water the bottom friction has a larger effect than during high water. Thus, the through of the tidal wave will be more slowed down than the crest, which also result in tidal asymmetry.

Since the tidal bore has to propagate against the river flow, a low river discharge is in favour for the formation of a tidal bore. The propagation speed of a tidal bore can be derived from the equation of a hydraulic jump. If the tidal bore does not change over time the following equation can be used to derive the speed of the bore,

$$c = -v_1 - \frac{\sqrt{g d_2 - d_1}}{2d_1} \tag{1.3}$$

Where the definitions are given in Figure 1.1. From this equation, it can be seen that a low river discharge (v_1) is in favour to get bore propagate against the river flow.

Thus, the formation of a tidal bore depends on multiple factors. The balance between the forcing and the bathymetry for the formation appears to be very fragile [3]. A small change in the forcing can disturb this

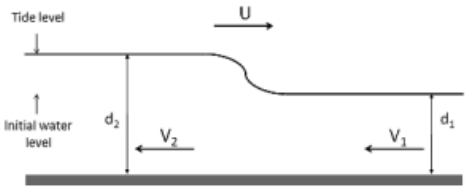

Figure 1.1: Sketch of a hydraulic jump. The water depth before and after the hydraulic jump are given by respectively d_2 (tide level) and d_1 (initial water level). The velocity before and after the jump are given by v_1 and v_2. The speed of the bore is given by U. [6].

balance. There are some examples of tidal bores which have disappeared after damming or dredging of the river [3]. This also applies for the Sittaung river as was mentioned by the Irrigation Department of Myanmar. In the past the tidal bore reached further upstream than nowadays. This could be caused by the damming of the Sittaung river, whereby the river discharge is changed significantly (see Figure 2.4). Only this hypothesis is never checked for the Sittaung River. The changes of the tidal bore in the Sittaung River could also be caused by changes in the bathymetry over the last years.

In general there is not much knowledge about the relation between the forcing, bathymetry and geometry of an estuary for the occurrence of a tidal bore. This is because the formation of a tidal bore depends on processes on different scales. The bore has a spatial scale of several meter whereas the formation of the bore depends on the scales of the estuary, which is in the order of 10^4 m. Lanzoni [7] showed that the tidal wave for an estuary can be classified based on two dimensionless parameters. The dissipative parameter (the relative intensity of friction to inertia) and the convergence parameter (the channel convergence relative to the oscillations of the free surface). A large dissipative parameter is necessary for the occurrence of a tidal bore, because than the propagation becomes non-linear resulting in deformation of the tidal wave [8]. Bonneton [9] goes one step further and approximated the dissipative parameter in large scale estuary variables specific for the formation of a tidal bores. This results in the following dimensionless parameter,

$$D^* = C_f * A_0 * L_{b0} / D_0^2 \tag{1.4}$$

Where D^* is the dissipative parameter, C_f Characteristic friction coefficient, A_0 tidal amplitude at the mouth, L_{b0} convergence length and D_0 the characteristic water depth. This formula can only be used to characterise the estuary. It is not possible to quantitatively describe the formation of a tidal bore [9]. However, the formula shows the influence of the water depth, bottom friction, tidal range, and funnel shape on the formation of a tidal bore. In this study the effects of the bathymetry and forcing are studied for the Sittaung River.

To do this a numerical model, Delft3D-Flow, will be used. Multiple researches used numerical models to study the hydrodynamics of a tidal bore. For the propagation of a tidal bore mostly depth-averaged models are used. Pan et al. used a 2D numerical finite volume method[10][11] for the Qiantang river and Liang et al. used a 2D hydrodynamic finite difference model for the Severn estuary [12]. For the details of the tidal bore often 3D models and Smoothed Particle hydrodynamics are used [13]. Delft3D-flow is never used to simulate the propagation of a tidal bore. The difference between Delft3D and the mentioned models is the numerical discretisation. In Delft3D a staggered conservative scheme for every Froude number is implemented for application of radpidly varying flows [14].

The region of the Sittaung river is not well developed. There is not much navigation or economic activity at the Sittaung River, which do not cause the tidal bore to be a problem. Only there is a lot of erosion at the mouth of the Sittaung River and it is assumed that this is caused by the tidal bore. However, this is not based on any measurements or physical arguments. Since a tidal bore is an impressive phenomenon, erosion problems can easily be assigned to it. There is indeed a lot of erosion/sedimentation at the mouth of the Sittaung River, which is visible at the Aqua-monitor [15]. Multiple villages have to be removed to prevent flooding. Some studies show that a tidal bore and the turbulence generated by the bore could have much effect on the sediment process [16][3]. There is never checked whether this is the case for the Sittaung River.

1.1. OBJECTIVE

The objective is to get insight in the influence of river discharge, bottom friction, tidal range and bathymetry on the tidal bore. The results are used to obtain some information about the erosion effects of the tidal bore. This results into multiple objectives. The first objective is:

- Simulate the tidal bore using a 2D numerical flow model

Subsequently the following objective is formulated:

- Simulate different scenarios and compare the results with the data.

To check the effect of the tidal bore on the erosion. The following objective is stated,

- Analyse the results to get insight in the erosion of the tidal bore.

2

MATERIAL AND METHOD

2.1. MATERIAL

The following datasets were used:

- *Water level measurements:* From four locations the water level is daily measured at 6:00AM, 12:00AM and 6:00PM. This data is collected by the Irrigation Department. This is done for a period from 2011 till 2014. In Figure 2.1 the locations of the measurements are shown. It must be note that this is not a complete dataset. At some months the discharge is missing for a few days and sometimes even for all the days.

- *Bathymetry profiles of cross-sections:* At five locations at the Sittaung River the bathymetry for a cross-section is measured in 2015. The data contains several points with the elevation (relative to mean sea level) and the corresponding horizontal distance from the centre of the river. In Figure 2.1 the locations are shown. This is a dataset from the Irrigation Department. In appendix C the bathymetry of the cross-section is shown.

- *Discharge measurement:* This dataset contains the daily mean discharge from 1996 till 2010. This is measured at the village Madauk. It is most likely that the data is obtained by using a q-h relation. This location is shown in Figure 2.1. This data is collected by the Irrigation Department.

- *Coastal model Myanmar:* A Delft3D model [17] [18] of the coast of Myanmar is available. This model includes the Gulf of Martaban and the Ayeyarwady delta. This model is mainly made for the Ayeyarwady delta, but also contains the whole estuary of the Sittaung river.

- *Navigation charts from Navionics:* Marine charts of the Navianions Webapp [19] contains bathymetry charts. These charts are based on depth measurements of ships owners.

- *IHO tidal observation stations:* The IHO datset contains the time-series of water level at multiple locations in the world.

- *SRTM digital elevation map:* The SRTM [20] digital elevation map contains the bathymetry collected by the Shutle Radat Topograpy Mission. The map contains bathymetry data with a resolution of 30-arc second.

- *Landsat:* The Landsat [21] maps contains satellite imagery of the earth. The images from Landat 8 were used. The accuracy is given by a 12 meter circular error with a 90-percentage confidence.

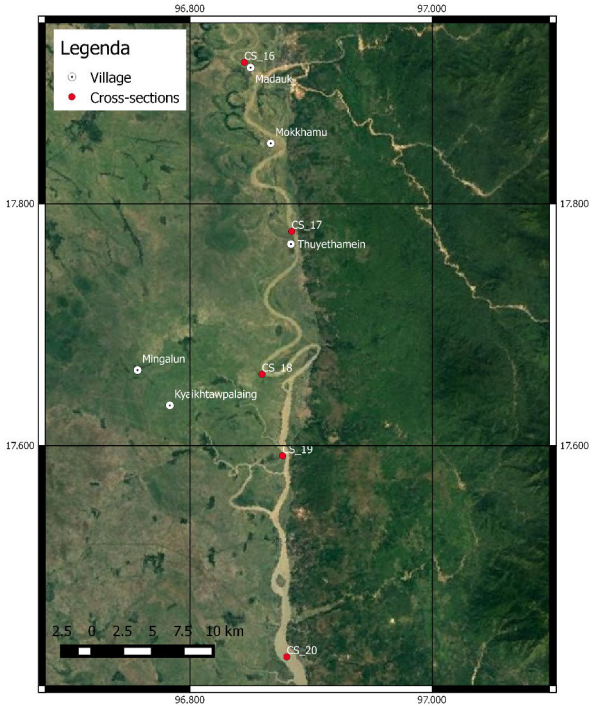

Figure 2.1: The location of Gauge stations for the water level, the location of the cross sections and the location of the discharge data.

To generate, analyse and visualise the results the following software programs are used:

- *Delft3D:* The numerical model Delft3D-FLOW was used to do the simulations.
- *Open Earth Tools:* The MATLAB scripts from the Open Earth Tools (Deltares) were used to analyse the results from Delft3D.
- *Delft3D-dashboard:* This tool was used to collect data about the tidal IHO stations and obtain the corresponding observation points.
- *QGIS:* QGIS 2.8.3 was used to analyse the results and to make visualisation of the results.
- *Python:* Python 2.8 was used to process the data and make various figures.

2.2. FIELDWORK

The Sittaung River was visited two times. The intention of the first visit was to get insight in the region and to obtain information about the tidal bore. During the second visit the depth was measured for a part of the river and it is tried to observe the tidal bore. At both trips a staff member of the Irrigation Department joined.

During the first trip three villages near the Sittaung River were visited (Kyaik Ka Thar, Moka Pa Lin and Thein Za Yat). In Figure 3.1 the locations of these villages are shown. The trip took place on 22-11-2016. At the villages questions about the water depth, existence of the tidal bore, the height of the tidal bore and the days when the tidal bore occur were asked. Besides of the questions also pictures were taken to get an idea about the bathymetry.

During the second trip depth measurements were carried out. The measurements were carried out at 30-11-2016 between 14:30 PM (UTM+6.5) and 17:00PM (UTM+6.5). The depth was measured for several points at the estuary with an echo sounder (Garmin echoMAP 42dv). The echo sounder uses a 77kHz sonar to measure the depth. The boat could only sail in the deeper parts of the river. Thus, it was not possible to obtain a complete cross section. Due to the fact that there was not a bench mark nearby as reference level one meter is added to the data to obtain the depth relative to mean sea level. During the period of the measurements, it was low water. This one meter is based on the tidal range near Kyaik Ka Thar, which is estimated during the fieldwork. The river bank near Kyaik Ka Thar has been seen during low and high water. The difference between high and low water is approximately two meter (see Figure A.1 of appendix A). At the start and end

of the measurements two locations were measured which are close to each other. The difference between the depth of both locations was very small ($\pm 20cm$). Therefore, it is assumed that the water level did not changed much during the measurement period.

2.3. MODEL SET-UP

This chapter contains the settings for Delft3D which was used for the simulations.

2.3.1. DOMAIN AND GRID

The land boundary is based on the Landsat data from 2016. A land boundary was constructed following the coastline and Sittaung River to create a domain. A curvilinear grid is constructed within the land boundary. The position of the intertidal area's and the main river was taken into account in such a way that the main flow is aligned with the grid cells. The small side channels ($\pm 50m$) were neglected in the grid. This can be done, because these small rivers have not a large effect on the propagation of the tidal bore. The storage of water inside these side channels is very small compared to the discharge in the main river. Therefore, the side channels have not much impact on the river discharge and thus the tidal bore. The open boundaries are located far from the area of interest to minimize the effect of errors from the boundary condition. This results in a grid started just downstream of Madauk and ends at the Andamanse Sea. In the region where the tidal bore propagates the grid size must be very small to simulate the large water level gradient. The grid size is $\pm 15m$ (in flow direction) in the area of interest. To reduce the computational time the grid sizes increases towards the sea boundary. This means that not all the coastal features can be included in the model. Since this is far away from region where the tidal bore propagates ($\pm 50km$), it will not result in inaccurate results. A few dry points were added to fit the model domain with the land boundary. The Yangon River and the area around Mawlamine are included in the domain in such a way that the two IHO tidal station falls inside the grid. Thus, a time series can be created for these locations to compare it with the IHO data. The final grid can be seen in Figure 2.2. The dry points can be seen in Figure B.4 and B.5 of the appendix.

The final grid is checked for orthogonality, smoothness and aspect ratio. The orthogonality of the grid is smaller than 0.02 in the area of interest and smaller than 0.24 in the whole domain. The aspect ratio is around 5 in area of interest. This is a relative high value, but because the grid cells are aligned with the main flow direction this is acceptable. The smoothness is smaller than 1.2 in the area of interest. These values fall within the quality criteria of the Delft3D-flow manual [22].

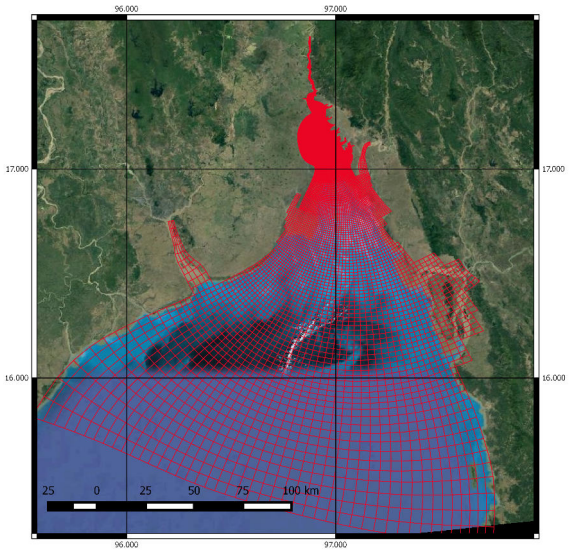

Figure 2.2: The final grid. Total number of grid cells: 71693; cells in m direction: 93; cells in n direction: 1505 and number of dry points: 75

2.3.2. BATHYMETRY

The bathymetry is based on multiple datasets. The grid can be divided into three parts. The river, the estuary and the Gulf of Martaban. For every part a different approach and datasets were used to obtain the

bathymetry. The depth points for the different parts can be seen in Figure B.1 of the appendix.

The bathymetry of the Gulf of Martaban was determined based on the Navioncs Webapp [19]. The navigation charts from this website were loaded into QGIS using geo-referencing. A shape-file containing the depth was created in QGIS from this map.

The bathymetry of the river part was created by using three datasets. The various cross-sections, the depth obtained from the fieldwork and the SRTM map. The data of these three datasets is shown in Figure 2.3. From this figure can be seen that there is a lot of scatter in the data. This scatter cannot be caused by the tidal influence. The tidal signal is verified for every dataset by checking the tidal table for the different dates and times. All the cross-sections were measured during low or slack water. The measurements during the fieldwork were also carried out during low water. Thus, all the measurements were carried out during low or slack water. Due to the large amount of scatter the SRTM data was used to determine the bottom slope, whereas the cross-sections were used to determine the cross-sectional profile. It is assumed that the water level has the same slope as the bottom level (equilibrium depth in the river). This is not entirely true due to the tidal influence, but it gives a good estimation. The water level difference between two points of the river is divided by the distance between these points. The effect of the tidal wave inside the river is taken into account by selecting the points upstream of the tidal wave. The tidal wave was clearly visible in the SRTM picture as a sudden increase of the water level over a short distance (see Figure B.7 of the appendix). This result in a bottom slope of 5e-5. At the location of the depth measurements the averaged depth is known. From this point the bathymetry increases with a slope of 5e-5 m/m towards the upstream boundary.

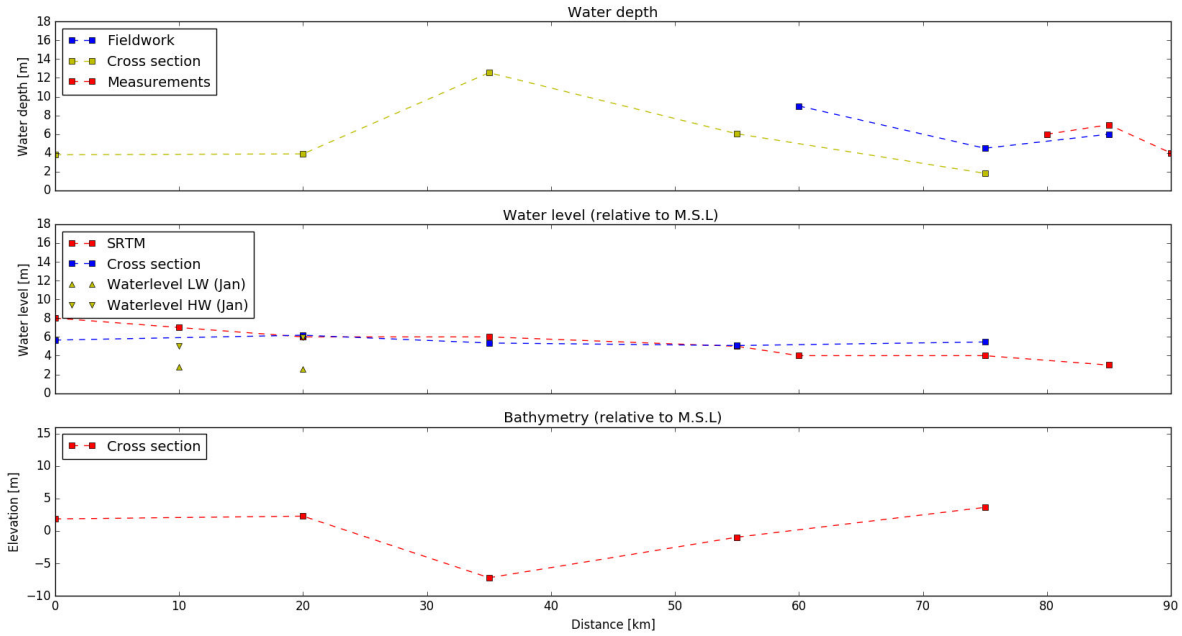

Figure 2.3: Bathymetry, water level and water depth for the Sittaung River. The distance is measured from Maudauk. The water depth for both the cross section and the measurements were collected during low water. The water level from two measurements in January are included in the picture. The water depth of the cross section is the difference between the water level and the mean water depth.

No data was available for the last part (the estuary). The Landsat images of November 2016 were used to obtain the locations of the intertidal areas. The depth at the intertidal areas is estimated from the pictures taken during the fieldwork. During the depth measurements it was low water and thus the intertidal areas where visible. The same depth was used for all the intertidal area's. The depth of the main channel is obtained by linear interpolate between the depth measurements (at the river part) and the depth from the Navionics charts (at Gulf of Martaban). The depth is adjusted multiple times for this region during the calibration. The final bathymetry can be seen in Figure B.3 of the appendix.

2.3.3. TIME STEP AND SIMULATION PERIOD

The staggered conservative scheme was selected as the advection scheme for momentum (see section 2.3.5). This means that the model is not unconditional stable. For stability the flow Courant number should be smaller than 2 [14]. The flow Courant number is given by,

$$\sigma = \frac{u\Delta t}{\Delta x} = 2 \tag{2.1}$$

Where σ is the Courant number, u the velocity, Δt the time step and Δx the grid size. With a velocity of 5 m/s and a grid size of 10 m this gives a time step restriction of,

$$\Delta t \approx \frac{2x10}{5} \approx 4sec \tag{2.2}$$

Four simulations with different time steps were done to check the effect of the time step on the accuracy. For two locations (see Figure B.5 of the appendix for the locations) the difference of the time series between two time steps was computed. The results can be seen in table 2.1. The simulation with a time step of 0.5 min is not stable and therefore the difference between 0.1 and 0.5 min can not be computed. For the other time steps the results are very similar, which would imply that a time step of 0.1 minute is suitable. Only due to the simulations where the parameters will be varied, the velocity could increase significantly. Especially when the river discharge is increased the velocity will increase. Therefore, a time step of 0.05 minute is chosen.

Observation point: Estuary 1		
Time steps [min]	**MSE water level**	**MSE v velocity**
0.5 - 0.1	Unstable	Unstable
0.1 - 0.05	1.94e-2	2.84e-3
0.05 - 0.025	1.37e-2	1.27e-3
Observation point: Tidal flat 1		
Time steps [min]	**MSE water level**	**MSE v velocity**
0.5 - 0.1	Unstable	Unstable
0.1 - 0.05	1.04e-2	1.50e-2
0.05 - 0.025	1.78e-3	8.40e-3

Table 2.1: Comparison of the time steps.

The simulation period is from 30-11-2016 (UTM+6.5) till 02-12-2016 (UTM+6.5). During these days the Sittaung River was visited and the maximum tidal amplitude of the spring neap cycle falls inside this period. Thus, for these days the time at which the tidal bore arises is known, which makes it possible to also calibrate the boundary conditions.

2.3.4. BOUNDARY CONDITIONS

The model contains two open boundaries. The upstream boundary is a discharge boundary and the downstream boundary is a water level signal. The discharge was based on measurements near Madauk (see Figure 2.1 for the location). The discharge boundary is located just downstream of Madauk. The discharge is measured daily for a period of 1996 till 2010. For the two days of the simulation period the discharge is shown in Figure 2.4. From this figure can be seen that the discharge increases in time. This is probably due to the construction of several dams in the Sittaung River. The discharge which is shown in the figure is during the dry season. Stored water will be released during the dry season, resulting in an increase of the discharge for this period of the year. Therefore, the averaged value for 30 November and 1 December of the last 20 years was used as a boundary condition. This gives an upstream boundary of 1050 m^3/s. This values also corresponds with the monthly averaged discharge of November and December.

The water level boundary is derived from a coastal model. In the following part coastal model refers to the external model and tidal model refers to the model of the tidal bore. The model domain of the coastal model contains the Gulf of Martaban and the Andaman sea. From the coastal model the water level time series for five points at the location of the boundary of the tidal model were computed. These results can be seen in Figure 2.5. From this figure can be seen that the amplitude decreases from the East to the West at the boundary. This is due to the relative small depth at the west boundary in the coastal model (the tidal wave is also more deformed at the West boundary). In reality the depth is larger in this region and therefore the boundary conditions were based on the East and East-middle time series. Furthermore, the figure shows that

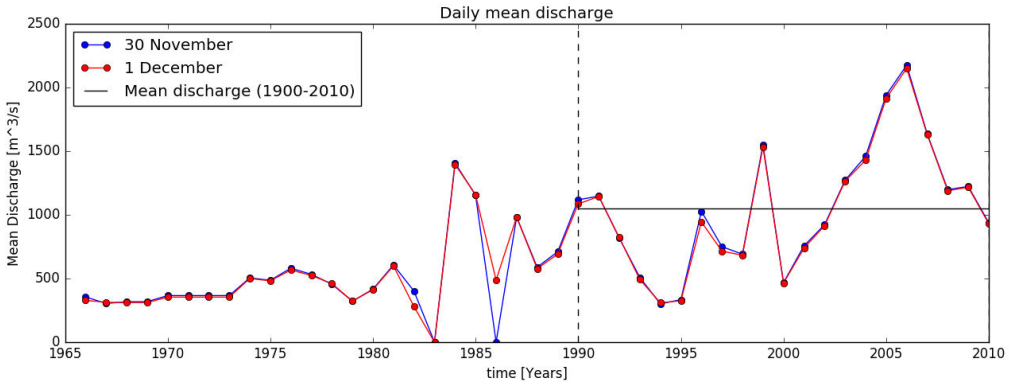

Figure 2.4: Daily discharge for 30 November and 1 December.

there is not a large phase difference between the East and West time series. Thus, one tidal signal can be used for the entire boundary. The tidal signal for the boundary is set as a combination of two daily harmonics. The daily double high water signal (D2) and daily quarter high water signal (D4). This is done because the tidal wave is already deformed when it enters the domain of the tidal model. The amplitudes for these signals were determined by comparing the tidal signal to the time series from the coastal model. This can be seen in the lower panel of Figure 2.5. The tidal signal is especially fitted to the second tidal wave on 30-11-2016. This is done because this is the largest tidal wave on this day. During the sensitivity analyse the other tidal wave on this days is simulated. This result in a D2 amplitude of 2.2 m and a D4 amplitude of 0.2 m.

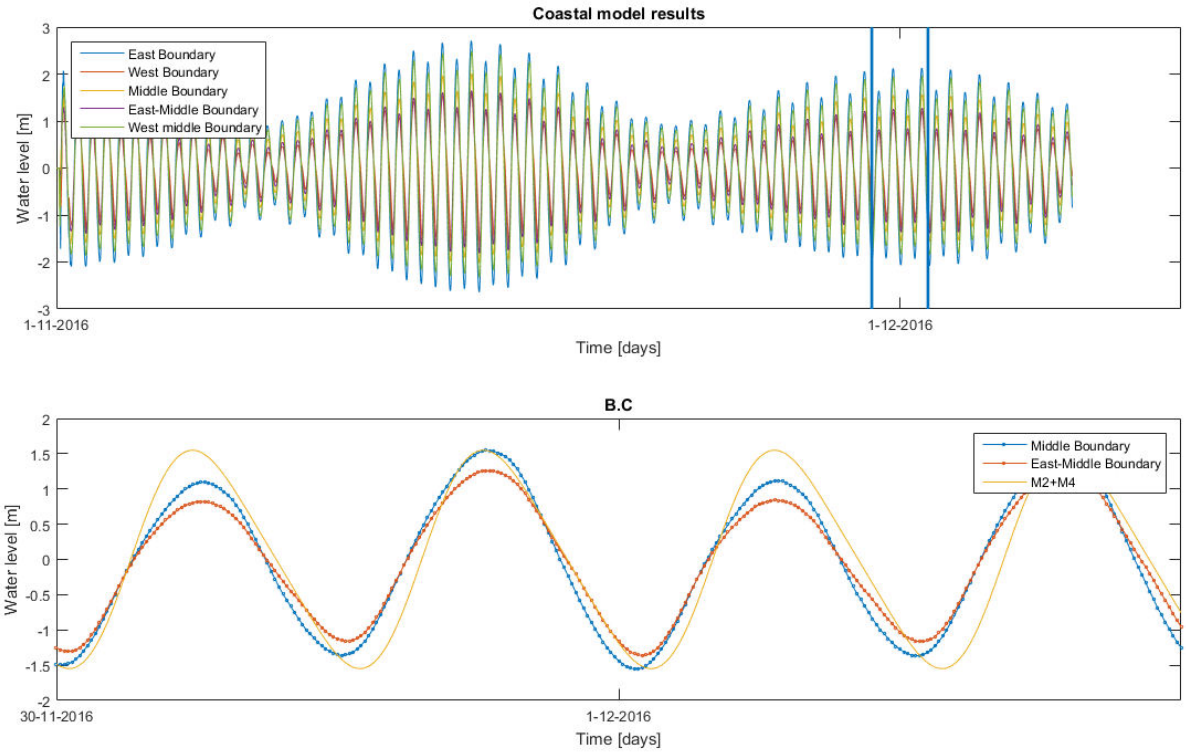

Figure 2.5: Coastal model results for the five observation points. The lower panel shows the boundary signal and two signals from the coastal model.

The phase of the D2 and D4 component was based on the two IHO tidal station in the domain (Amherst and Elephantpoint). The phase between D2 and D4 is not changed, which means that the D4 zero up-crossing

corresponds with a zero crossing of the D2 tide (see appendix Figure B.2). The phase is adjusted until high and low water corresponds with the IHO tidal stations. Elephant point is located in a very shallow region (inside the Yangon river) and therefore Amherst is more useful for the calibration of the phase. The model results correspond better to the signal at Amherst than at Elephantpoint as can be seen in Figure 2.6.

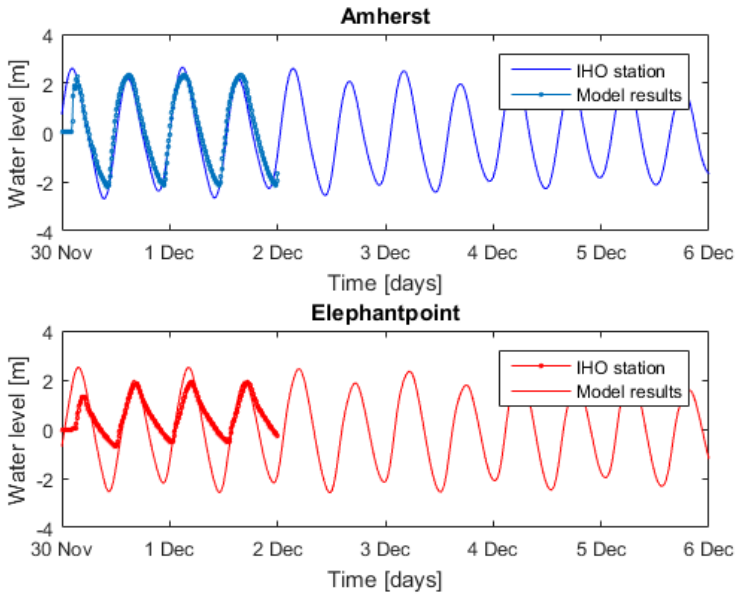

Figure 2.6: Model results compared to IHO tidal stations. the upper panel shows the Amherst signal and the lower panel the Signal from Elephantpoint.

2.3.5. NUMERICAL PARAMETERS

For the advection scheme of momentum multiple numerical schemes are implemented in Delft3D. A tidal bore causes a large water level gradient. Thus, the staggered conservative scheme was used for the simulations. This scheme is based on energy or momentum conservation (depending on flow contraction or expansion). Therefore, the scheme is suitable for rapidly varying flows [14]. The drawback of this approach is that the scheme is not unconditional stable. It requires a time steps restriction for stability.

Due to intertidal areas inside the model the flooding and drying parameters are important. The threshold depth for drying and flooding is set to 0.2 m. This means that if the water depth is lower than 0.2 m the grid is considered to be dry. Based on different simulations, it could be seen that 0.2 m represents the drying/flooding process well. Secondly, the tidal bore was analysed by looking where the water level changes are larger than 0.2 m within a short time interval (2.5 min). When the threshold depth would be set to a larger value the drying/flooding will affects these results.

2.4. CALIBRATION

The model was calibrated for two physical parameters: the bottom friction and the horizontal eddy viscosity. Most attention went to the bottom friction, because it is known that the bottom friction affects the tidal bore [8]. Furthermore, the regions where the bathymetry is unknown were calibrate. The calibration was based on the propagation of the tidal bore. This is made visually by looking at the difference in water level between a short period (2.5 min). If the water level changes are larger than 0.2 meter, than it is assumed that the tidal bore has propagate through the grid cell. The time steps of the first tidal waves were skipped, because the propagation of the tidal bore is not realistic due to the flat initial water level. The results for the bottom friction and the horizontal eddy viscosity can be seen in Figure 2.7. From these results was concluded that a Chezy coefficient of 70 $m^{1/2}/s$ gives the best results. The tidal bore did not propagate further than Kyaik Ka Thar in this simulation. The horizontal eddy viscosity does not have much effect on the propagation and thus the default value of 1 m^2/s was selected. The calibration of the depth was done because the results did not correspond entirely with the field observations. The tidal bore disappeared in a part of the domain (directly after the bend in the estuary). There were done multiple simulations where the bathymetry is changed. The

height of the intertidal area was changed to obtain a simulation where the tidal bore only propagates through the main channel. The depth of the main channel was also adjusted to a profile which can be expected based on the cross-section. The outer bend was made deeper than the inner bend.

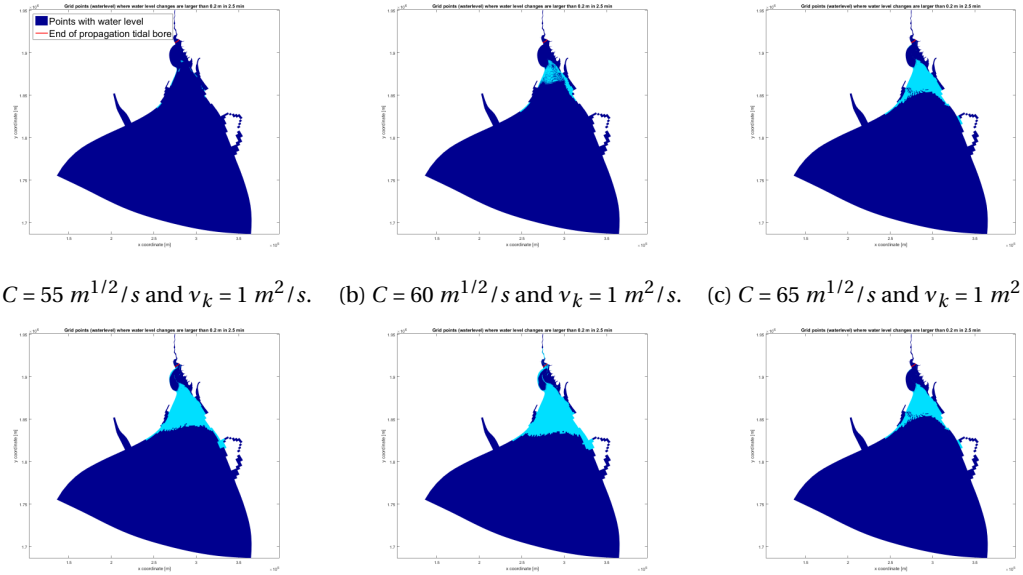

(a) $C = 55\ m^{1/2}/s$ and $\nu_k = 1\ m^2/s$. (b) $C = 60\ m^{1/2}/s$ and $\nu_k = 1\ m^2/s$. (c) $C = 65\ m^{1/2}/s$ and $\nu_k = 1\ m^2/s$.

(d) $C = 70\ m^{1/2}/s$ and $\nu_k = 1\ m^2/s$. (e) $C = 75\ m^{1/2}/s$ and $\nu_k = 1\ m^2/s$. (f) $C = 65\ m^{1/2}/s$ and $\nu_k = 10\ m^2/s$.

Figure 2.7: Results for different parameter settings. Regions where the water level changes are larger than 0.2 meter within 2.5 minutes are shown in light blue. The turbulent viscosity is shown as ν_k and the Chezy coefficient is shown as C.

2.5. OVERVIEW PARAMETER SETTINGS

In the table below the final settings are shown.

Latitude	17 deg
Orientation	0
Start simulation	30-11-2016
End simulation	02-12-2016
Time step	0.05 min
Time zone	6.5 hr
Initial condition water level	0 m
River boundary	1050 m^3/s
Sea boundary components	D2, D4
D2 amplitude	2.2m
D4 amplitude	0.2m
D2 phase	-13.8728 degree
D4 phase	168.7457 degree
Water density	1025 kg/m^3
Gravity	9.81 m/s^2
Chezy coefficient	70 $m^{1/2}/s$
Horizontal eddy viscosity	0.1 m^2/s
Threshold depth	0.2
Advection scheme for momentum	flooding

Table 2.2: Model parameters settings

2.6. VERIFICATION

The model results were checked with the relation between cross-sectional area and tidal prism. According to the work of O'Brien the relation between the equilibrium cross-section of a tidal inlet and the tidal prism is given by [23],

$$A_{eq} = cP^q \tag{2.3}$$

Where A_{eq} is the equilibrium cross-section of the channel measured below MSL, P the tidal prism and q, c coefficients. The value of the coefficients q is found to be around 1 and the value of the coefficient c lies in a range from $10^{-4} - 10^{-5}$ [5]. It appears that the above relations also holds along the channel [24]. To check whether this also holds for this simulation, the tidal prism and cross-sectional area were computed for different cross-sections. The cross-sectional area is the area below mean sea level. The tidal prism is the integral of the last ebb period of the simulation to exclude the spin-up effects. The integral boundary starts from the last down crossing till the following up-crossing of the discharge time series. The results can be seen in Figure 2.8. A power function is fitted through the data points. The power is close to 1, which shows that the model bathymetry and geometry corresponds with the tidal prism.

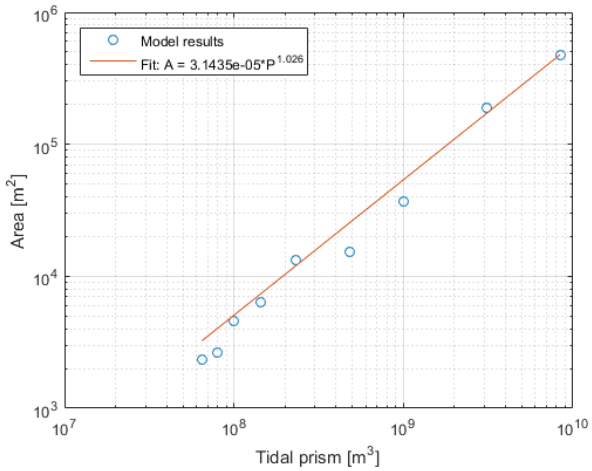

Figure 2.8: Tidal prism plotted against cross sectional area for different cross sections. The blue circles shown the results from the model and the red line is a regression line through the points. The equation of the regression line is shown in the legend.

2.7. SENSITIVITY ANALYSE SET-UP

For different scenarios the model was applied. Four simulations were done where the Chezy coefficient was varied with $+/-10\%$ and $+/-20\%$. The river discharge was varied with -50%, $+100\%$, $+200\%$ and $+300\%$. These values correspond with the various river discharge in the different seasons. In February till May the river discharge is reduced by 50% and for the months July and October the river discharge is 100% larger. Furthermore, the river discharge was reduced by 50% before the construction of the dams. During the rainy season the river discharge is on average 200% larger and it can increase to 300% for some days. The tidal range was varied for the different amplitudes which occur during a year. The ratio between the D2 and D4 amplitude is kept the same. The following amplitudes were modelled: 2.0 meter for the other amplitude on 30 November 2016, 1.5 meter for the minimum amplitude in the spring-neap cycle and 3.5 meter for the maximum amplitude during the year. The amplitudes for both D2 and D4 are shown in the table 2.3. To see the effect of the water depth on the tidal bore the bathymetry was changed. This is done by adding a uniform value to the bathymetry for the upper part (see Figure B.6 of the appendix for the bathymetry). This means that only the depth of the river and estuary is changed. To prevent a step in the bathymetry, the transition region is smoothed. The bathymetry is changed by -1, -2, +1 and +2 meter.

Total amplitude	M2 amplitude [m]	M4 amplitude [m]
2.0	1.83	0.16
1.5	1.375	0.125
3.5	3.21	0.28

Table 2.3: Tidal amplitude for different simulations.

3

RESULTS

3.1. FIELDWORK

In the following sections the results from the fieldwork are described.

3.1.1. FIELDWORK 1

From the first village it became clear that the tidal bore only occurs a few days after full and new moon. The other information collected during this trip is shown in the table below and in appendix A. The data of the water depth is also shown in Figure 2.3. Besides of the location of the tidal bore also visual information (pictures) about the bathymetry were collected. From the visual information the locations of intertidal areas were determined. In appendix A pictures of the three villages are included.

Village	Depth (low water) [m]	Height Tidal wave [m]	Intertidal area's	Figure
Kyaik Ka Thar	6	9	Yes	Figure A.1
Moka Pa Lin	4.5	-	No	Figure A.2
Thein Za Yat	10	2.5	No	Figure A.3

Table 3.1: Results fieldwork 1.

3.1.2. FIELDWORK 2

An overview of the locations of the fieldwork is shown in Figure 3.1. The depth is obtained for the red line in the figure (track of the boat). It must be noticed that the bathymetry of this part can change within a few months. The fisherman told that different sand banks were not visible a few months ago. Thus, these results give a general idea about the depth in this region. An averaged depth for a transect of the estuary can be seen in Figure 2.3.

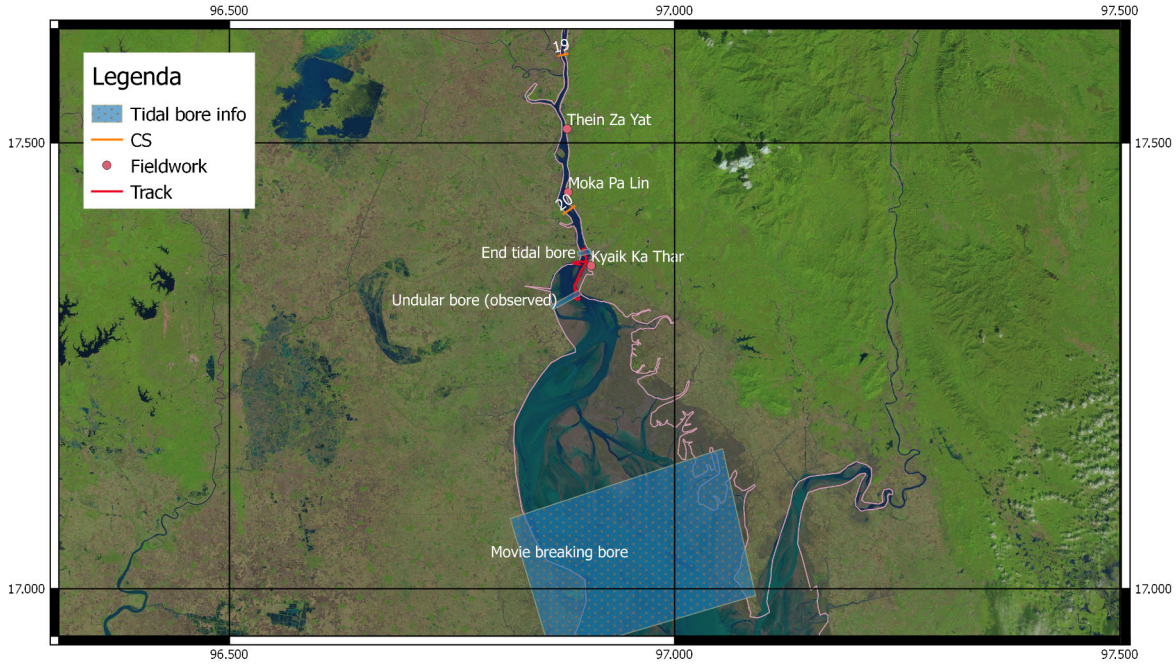

Figure 3.1: Map of the villages visited during the fieldwork. The red line represents the path, which is sailed with the boat. The locations of the received bathymetry cross sections are shown as orange lines with the corresponding cross section number.

Besides of the measurements also the tidal bore was observed. First multiple waves entered the river, as can be seen in Figure 3.3. A few minutes later 1 undular bore passed by with a wave height of approximately 30 cm. It is expected that this wave is caused by a larger (breaking) tidal bore downstream. A video of the tidal bore proves that there is a breaking bore downstream. According to the local fisherman this video was taken at the village Zawtika (downstream of Kyaik Ka Thar), but there is no other information found which confirms this. The region around Zawtike is shown in Figure 3.1. These days it was not possible to go further downstream with the boat due to the tidal bore. The local fisherman could tell that it was not possible for small ships to sail 7 days after full/new moon downstream of Kyaik Ka Thar and 5 days for larger boats. Near Kyaik Ka Thar the tidal bore could be seen three days after full/new moon. This implies that the tidal bore must be larger more downstream of Kyaik Ka Thar. A few minutes after the undular bore, the flow velocity increased. The flood flow increased so much that the boat has to be wait near the bank. In Figure 3.2 the described information is shown in a time line with the tidal signal of two tidal station nearby.

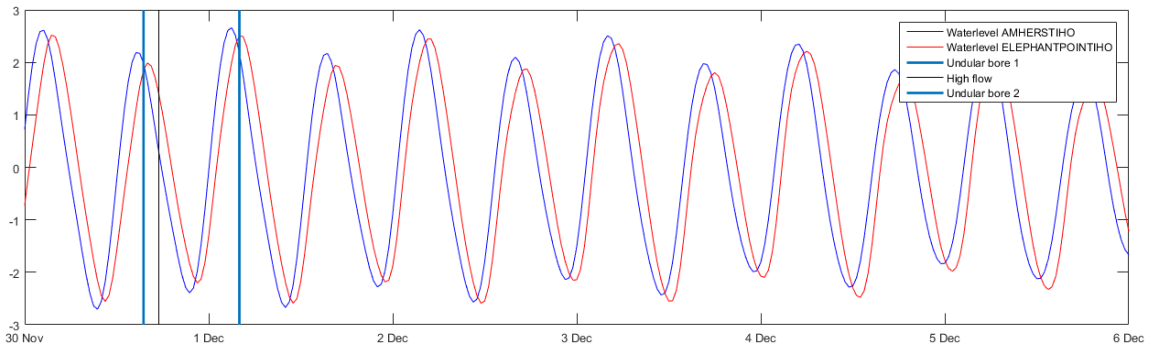

Figure 3.2: Tidal signal of two nearby IHO stations. The blue indicated the times where the tidal bore was seen and the black shown the point where the flood started in Kyaik Ka Thar.

Furthermore, the local fisherman showed until where the tidal bore could be seen (just upstream of Kyaik Ka Thar) and that there is a difference between the height of two tidal bores on a day. The tidal bore the next morning would be larger (around 1 meter). The next day the fisherman would show us the second (larger)

tidal bore with the boat. Unfortunately, this tidal bore was missed. The people from the village could hear the tidal bore around 4 AM.

Figure 3.3: Picture of the tidal bore near Kyaik Ka Thar (30-11-2016 UTM 15:30+6.5).

3.2. FINAL SIMULATION OF THE TIDAL BORE

In Figure 3.4 the water level changes, water level and initial bed level are shown for the final simulation. The water level differences are the change of water level within 2.5 minutes. The tidal bore can be seen in the upper panel as a large water level difference. For a transect along the estuary the water level and bed level are shown in the lower panel. The transect goes through the intertidal area and therefore a hill can be seen in the bed level (see Figure B.3 of the appendix). The tidal bore can be seen as a steep front in the water level. The height of this front corresponds with the water level changes in the upper panel.

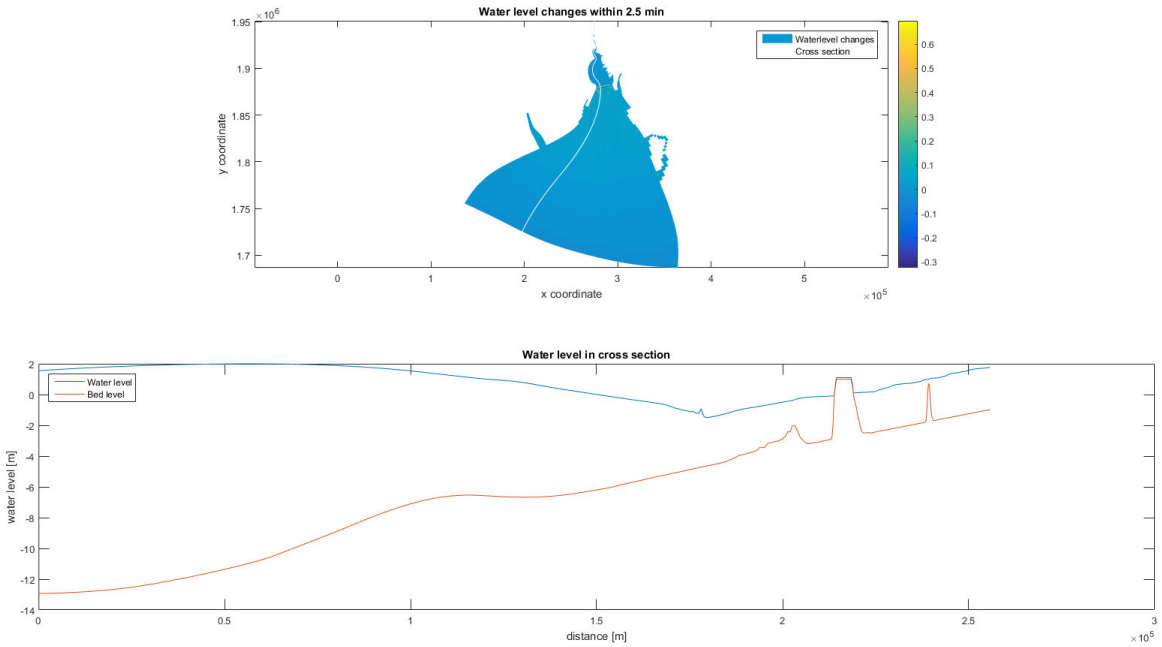

Figure 3.4: transect along the estuary

3.3. RESULTS OF SENSITIVITY ANALYSE

In the section below the results for the different simulations with varying Chezy coefficient, river discharge, tidal range and bathymetry are shown. The figure with the area of the tidal bore shows the grid points where water level changes are larger than 0.2 m in 2.5 minutes. The figure with the water level differences shows the maximum water level differences (in 2.5 minute) which occurs in the grid cells.

Chezy coefficient	Area of the tidal bore	water level differences
-20% $[56 m^{0.5}/s]$	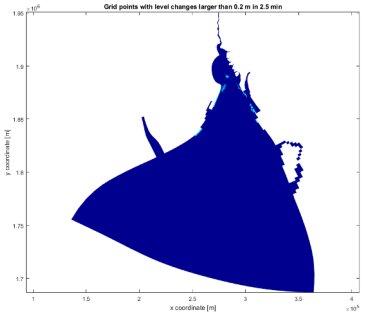	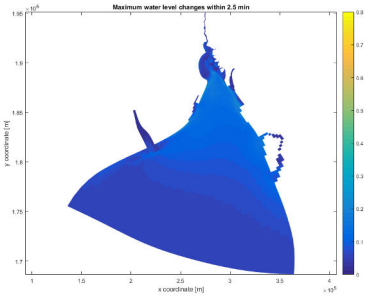
-10% $[63 m^{0.5}/s]$	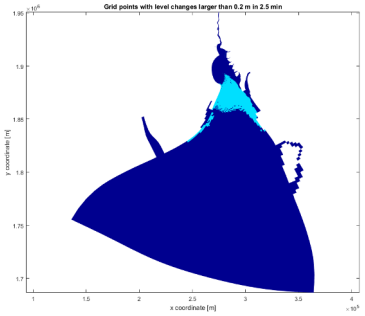	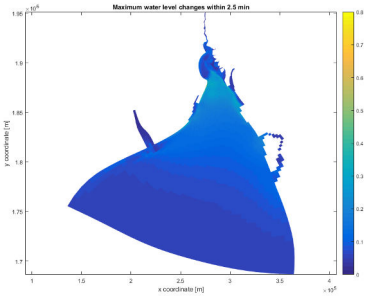
$+0\%$ $[70 m^{0.5}/s]$	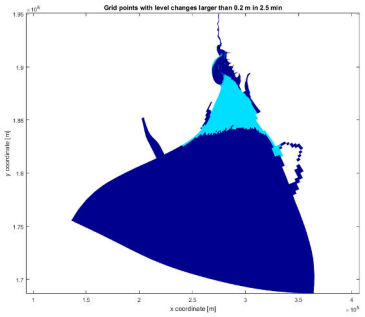	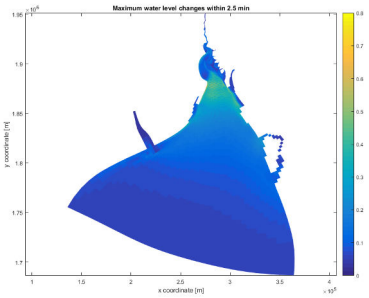
$+10\%$ $[77 m^{0.5}/s]$	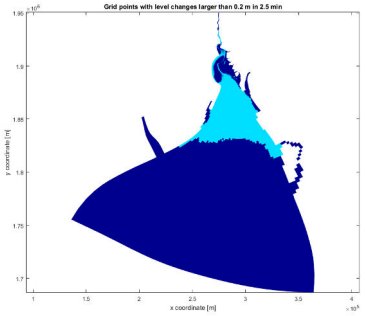	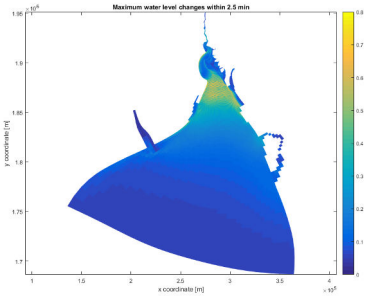
$+20\%$ $[84 m^{0.5}/s]$	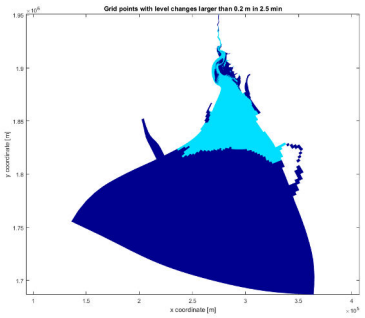	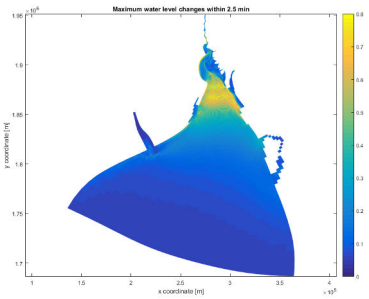

River discharge	Area of the tidal bore	water level differences
−50% $[525 m^3/s]$	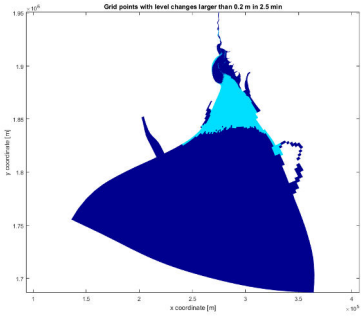	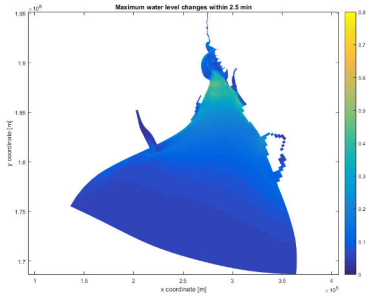
0% $[525 m^3/s]$	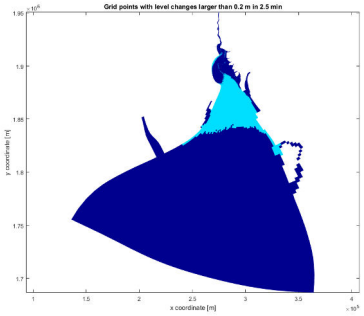	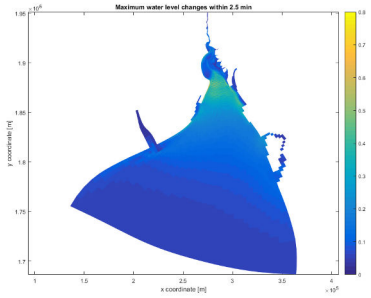
+100% $[2100 m^3/s]$	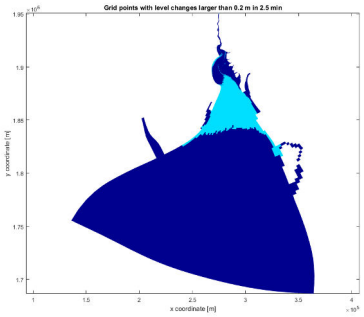	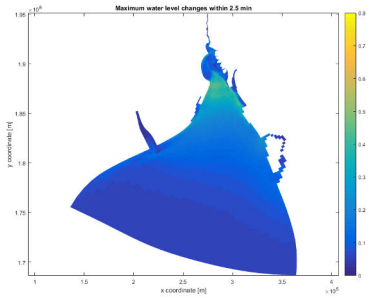
+200% $[3150 m^3/s]$	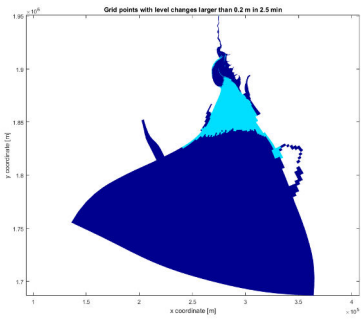	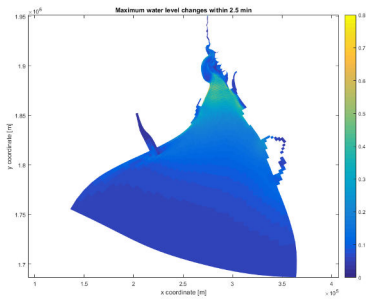
+300% $[4200 m^3/s]$	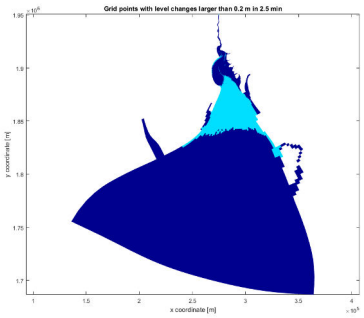	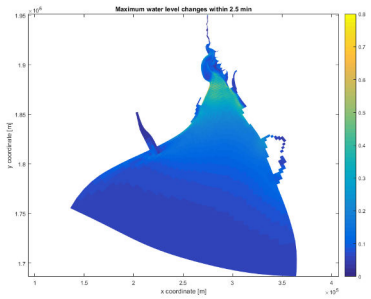

Tidal Amplitude	Area of the tidal bore	water level differences
1.5 meter	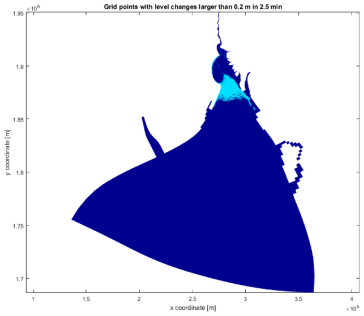	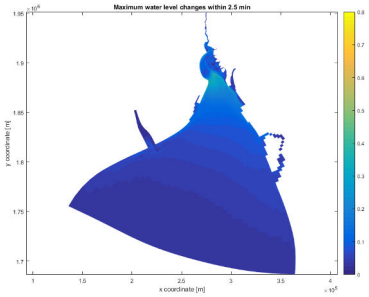
2.0 meter	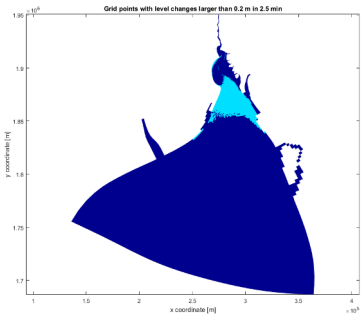	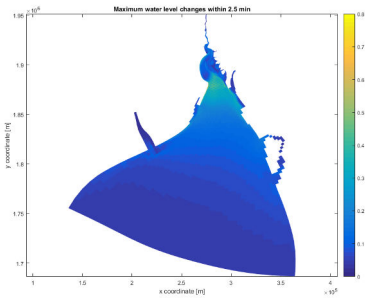
2.2 meter	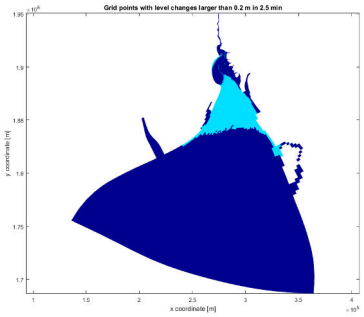	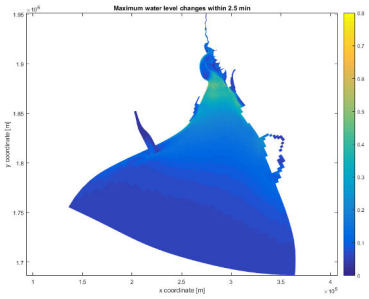
3.5 meter	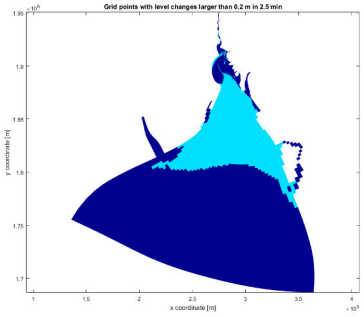	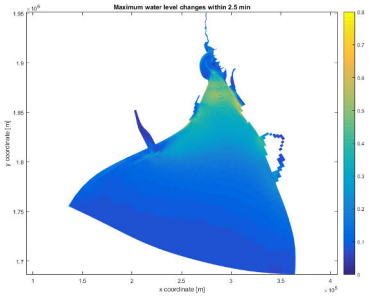

Bathymetry changes	Area of the tidal bore	water level differences
-2.0 meter	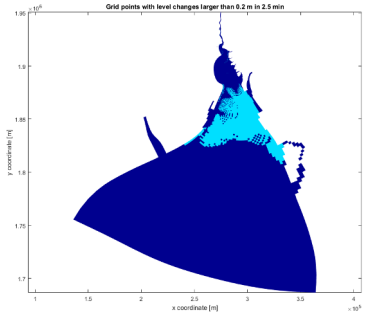	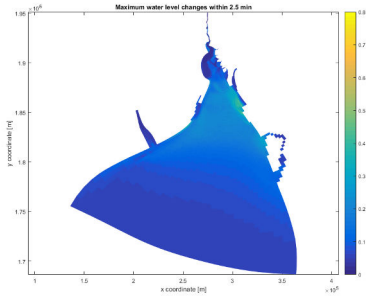
-1.0 meter	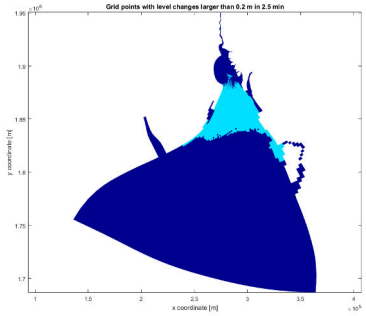	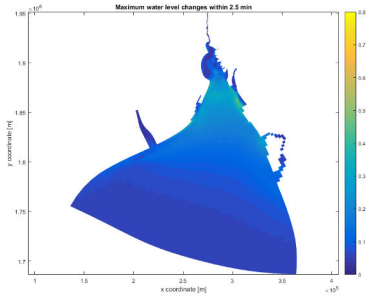
0.0 meter	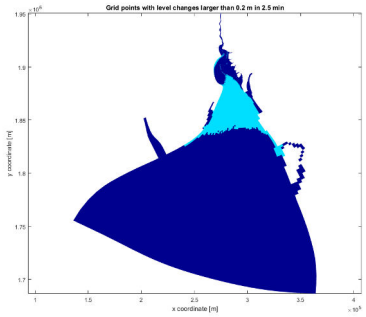	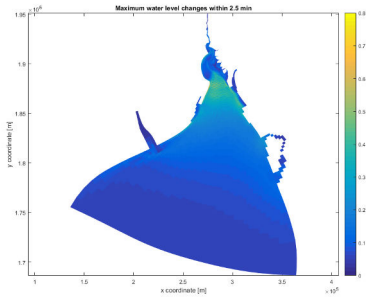
+ 1.0 meter	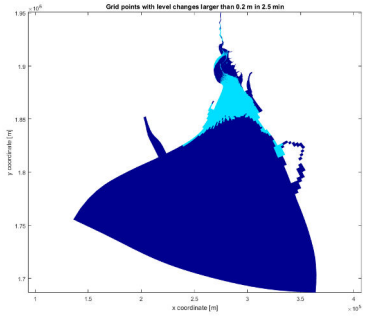	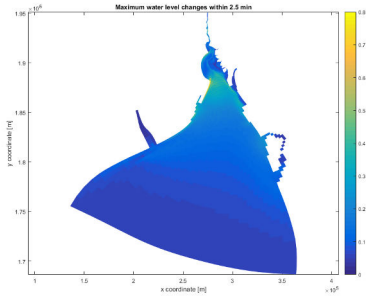
+ 2.0 meter	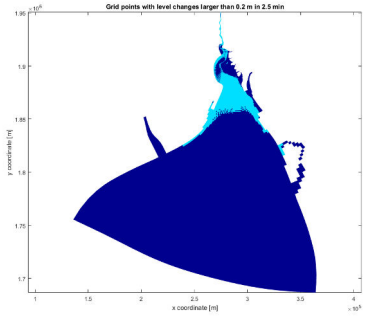	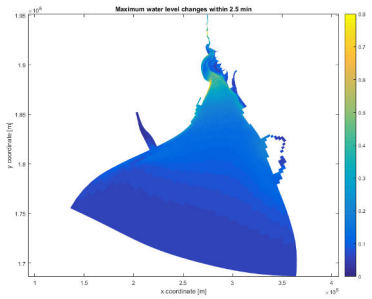

3.4. VELOCITY

In Figure 3.5a and 3.5b the velocity is shown for two simulations. A simulation with the tidal bore (Chezy coefficient of 70 $m^{0.5}/2$) and a simulation without a tidal bore (Chezy coefficient of 56 $m^{0.5}/2$). The figures only show the upper part of the model where the tidal bore propagates.

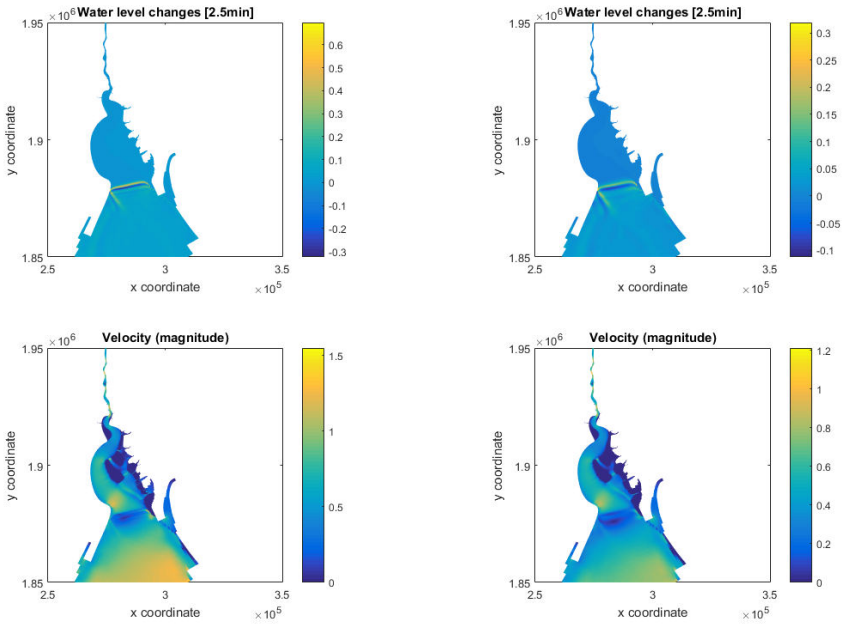

(a) Velocity magnitude for a simulation with tidal bore.

(b) Velocity magnitude for a for simulation without tidal bore.

4

Discussion

The results from the first field trip were not very useful except for the visual images of the region. Due to the difficulty of the communication the data is not very reliable. For example, the data of the tidal wave height in Table 3.1 was firstly interpreted as tidal bore height. After the second trip, it became clear that the tidal bore did not reach the villages Moka Pa Lin and Thein Zat Yat. Thus, it is assumed that this data is about the tidal amplitude. On the other hand, the information from the second trip was much more convincing. Thus, the information from the second trip was used in this study. The information received from the fisherman corresponds to the tidal signal of the nearby stations (see Figure 3.2). This figure shows a semi-diurnal tidal signal with daily inequality. The same information was obtained from the fisherman. Furthermore, the time at which the two tidal bores where observed corresponds to this signal.

The tidal bore can clearly be seen in Figure 3.4 as a disturbance in the water level. At this moment of time the water level changes are around 0.5 meter at the location of the tidal bore. This implies that the 2.5 minute time interval is short enough to capture the tidal bore.

From the results of the simulation of the tidal bore (see Figure 2.7d and 3.4) can be concluded that the tidal bore starts near the village Zawtika and then propagates for around 50 km. This does not entirely correspond with the information from the fieldwork. From the fieldwork it is known that the tidal bore propagates further upstream (to Kyaik ka Thar). In the model results, the tidal bore disappeared after the bend (y-coordinate of $1.87x10^6$) in the estuary and becomes visible again at the West bank of the estuary just before Kyaik Ka Thar. This difference could be caused by the fact that the height of the tidal bore is smaller upstream. The tidal bore could be damped too much in this area, causing the tidal bore to disappear. This extra damping can be the result of a lack of information about the bathymetry or due to the assumption of an uniform friction for the whole domain. The bathymetry of this area is not entirely known and the estimated depth could cause this difference. The bottom friction is assumed to be homogeneous for the entire domain but in reality this is not true (e.g. different vegetation and bottom soil).

The influence of the bottom friction on the tidal bore is very large. This means that the assumption of a homogeneous bottom friction could have signification effects on the tidal bore. For a more detailed simulation more accurate data of the bed properties must be used. Furthermore the results shown that a larger Chezy coefficient (less friction) is in favourable for the tidal bore. With a larger Chezy coefficient the tidal amplitude is damped less. Therefore, the tidal bore can propagate further upstream. For a bottom friction of 77 $m^{0.5}/s$ the tidal bore propagates all the way to Thein Za Yat. Besides of the propagation of the tidal bore, also the amplitude of the tidal bore increases for a higher Chezy coefficient.

The river discharge has less influence on the tidal bore. For all the four simulations the results are very similar. This implies that the seasonal variety of the discharge does not affect the tidal bore. Besides of the seasonal impact of the river discharge, there can also be concluded that the construction of the dams and thereby the change of discharge, do not result in much changes for the tidal bore. Thus, the changes on the propagation of the tidal bore for last year's cannot be caused by the damming of the river. Thus, the changing geometry of the estuary remains as cause for the changes of the tidal bore.

Similar to the bottom friction the tidal range is also an important factor for the occurrence of the tidal bore. This also corresponds with the occurrence of the tidal bore during the spring-neap cycle. Only a few days after full/new moon the tidal bore occurs at Kyaik Ka Thar. During neap tide the amplitude is 1.5 meter. From the results can be seen that for this amplitude the area where the tidal bore propagates is very small.

This does not entirely follow from the fieldwork results. It was stated that there is no tidal bore during neap tide. This difference can be caused by multiple factors. Firstly the data from the fieldwork is not correct for the downstream area. The fisherman based the information on their experience, but it is not clear how accurate this data is for the downstream region. Secondly, the difference can be caused by an inaccurate bathymetry and bottom friction in this region. At last the criterion for the occurrence (water level changes larger than 0.2 m in 2.5 minutes) of the tidal bore is to sensitive. The 2.0 meter amplitude simulations corresponds to the smaller tidal wave on 30 November caused by daily inequality. From the results can be seen that there is, as told by the fisherman, a difference between the two tidal bores on a day. The height of the bore is smaller, but also the region of propagation is smaller. Thus, a small difference in amplitude (0.5 m) can have large effect on the propagation of the tidal bore. The simulation with a tidal amplitude of 3.5 m shows the largest tidal bore which occur during a year. From the results can be seen that the tidal bore reaches much further upstream. Furthermore, the tidal bore occurs further downstream. This is not entirely correct, because in the results the tidal bore reaches the mouth of the Yangon river. It is known that there is never a tidal bore near the Yangon River. This difference could be caused by the same reasons as stated above.

Finally, four simulations are done with a different bathymetry. Just like the bottom friction and the tidal range the bathymetry is an important factor for the formation of the tidal bore. The tidal bore propagates much further upstream in the simulations where the bathymetry is changed by +1 and +2 meter. This is also expected because the shallow water effect for the tidal propagation becomes stronger. There are some differences at the location where the tidal bore starts to occur. These differences are caused due to the smoothing of the bathymetry. Thus, the bottom slope is not the same for every simulation.

It is very difficult to say something about the effects of the tidal bore on the erosion at the Sittaung estuary. From the results in Figure 3.5a and 3.5b can be seen that the difference in velocity is small for a simulation with and without a tidal bore. Thus, from these results it is impossible to describe the effects of the tidal bore on the erosion. A sub-grid approach is used whereby energy and momentum are conserved between the grid points, but details of the tidal bore are not included in the simulations. Therefore, the turbulence caused by the tidal bore is not visible in the results. However, from all the collected data some information of the erosion can be given. In the upstream part of the estuary the tidal bore is a small undular bore (see Figure 3.3). This bore will not have much effect on the erosion at this region. Furthermore, the tidal bore occurs only a few days in a month, which suggest that other processes are more important for the erosion rate. Downstream of the estuary the tidal bore is larger and could have more effect on the erosion. From the received video of the tidal bore in this region, the effect of the tidal bore on the bank is visible. Due to lack of data and information of this area this is difficult to confirm.

5

CONCLUSION

Data about the tidal bore is collected during two visits of the Sittaung River. This data is used to set-up a 2D numerical model of the tidal bore. With this model the effect of the bottom friction, river discharge, bathymetry and tidal range on the propagation of the tidal bore is studied.

The propagation of the tidal bore can be simulated with the Delft3D-flow model. The results correspond mostly with the collected data. However, due to the lack of data there is still some uncertainty in the results. It is certain that the tidal bore disappears near the village Kyaik Ka Thar. In the model results the tidal bore is already disappeared before Kyaik Ka Thar. The difference between the model results and reality will be caused by inaccuracies in the bathymetry and the bottom friction. Though, the general propagation of the tidal bore can be simulated. Therefore, it is also possible to change the parameters to do a sensitivity analyse on the propagation. From the sensitivity analyse can be concluded that the bottom friction, tidal range and bathymetry are the most important factor for the occurrence of the tidal bore. The river discharge has almost no influence on the propagation. Thus, the damming of the Sittaung River, which caused changes in the river discharge, cannot result in changes in the propagation of the tidal bore. If the river discharge is not responsible for the changes of the tidal bore in the last years, then this must be caused by the changed in the bathymetry. This also follows from the sensitivity analyse about the bathymetry. The changes in bathymetry have more effect on the propagation than the changes in river discharge. Secondly, this also imply that the variety during a year is only caused by the tidal range, because the river discharge and the tidal range are the only two parameters which vary during a year. The sensitivity analyse also shown that the tidal range has a significantly effect on the propagation.

The model results cannot be used to give a good estimation of the erosion, but from all the collected data a general view on the erosion can be given. The tidal bore is a small undular bore in the upstream part of the estuary. This would suggest that the tidal bore will not have much effect on the erosion. Downstream in the estuary the tidal bore is larger and could have more impact on the erosion. Due to lack of data it is hard to give a hard conclusion about the erosion in the estuary. For a more accurate prediction of the erosion a detailed study should be carried out.

A

APPENDIX-A: FIELDWORK

A.1. FIELDWORK

In Figure A.1 the bank of the Sittaung River near Kyaik Ka Thar can be seen. There are large intertidal area's at both side of the channel. During high water the water level is just below the dyke (±1.5 m).

Figure A.1: Intertidal area near Kyaik Ka Thar

In A.2 the bank near Moka Pa Lin is shown. At this particular place there is a problem with bank erosion. There are no intertidal area at this location. The difference between high and low water is approximately 2 meter.

Figure A.2: Bank near Moka Pa Lin

The bank at Thein Za Yat can be seen in Figure A.3. The villages is located at the river and therefore there is a concrete wall protecting the bank. Like Moka pa Lin there are no intertidal area at the place. During high water the water level reaches the wall (±1 m).

Figure A.3: Bank near Thein Za Yat

B

APPENDIX-B: MODEL SET-UP

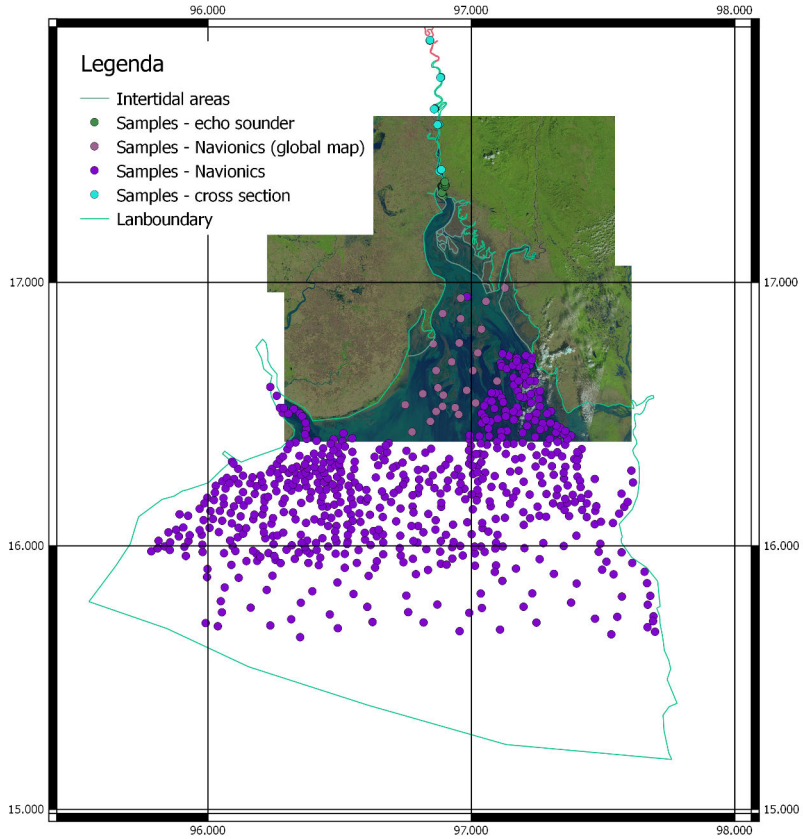

Figure B.1: Samples for the bathymetry

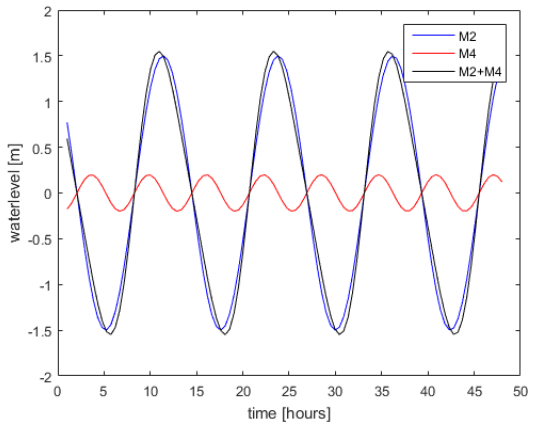

Figure B.2: M2 + M4 signal.

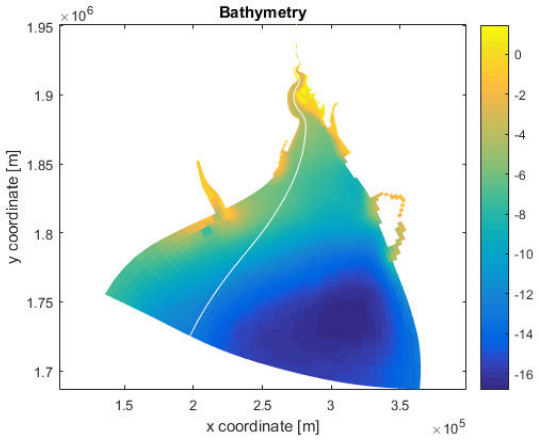

Figure B.3: Bathymetry.

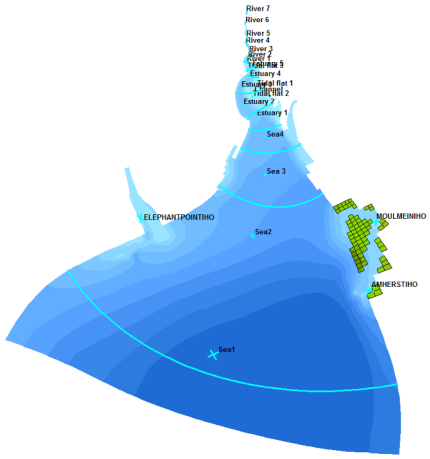

Figure B.4: Location of observation points, cross sections and dry points.

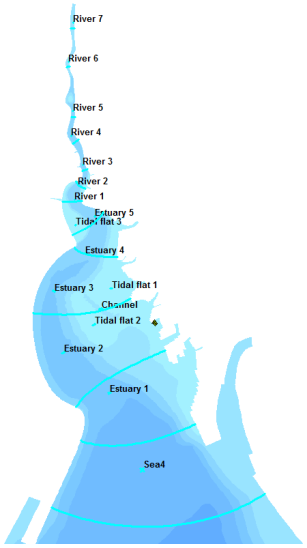

Figure B.5: Location of observation points, cross sections and dry points for upper part of the domain.

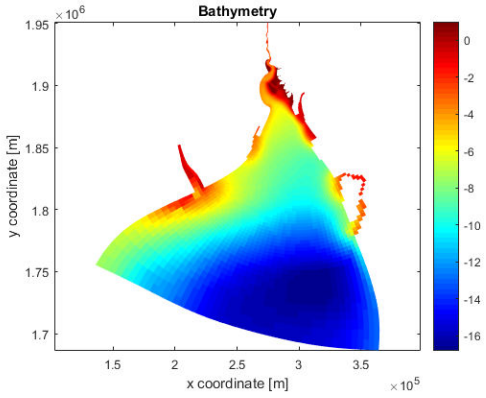

(a) Bathymetry where upper part is changed with -1 meter.

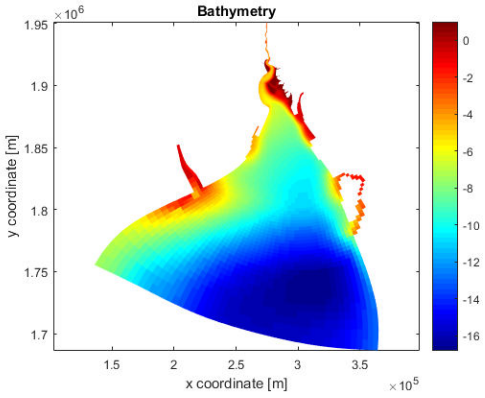

(b) Bathymetry where upper part is changed with -2 meter.

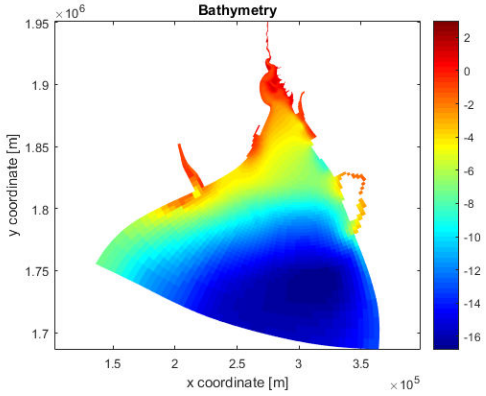

(c) Bathymetry where upper part is changed with +1 meter.

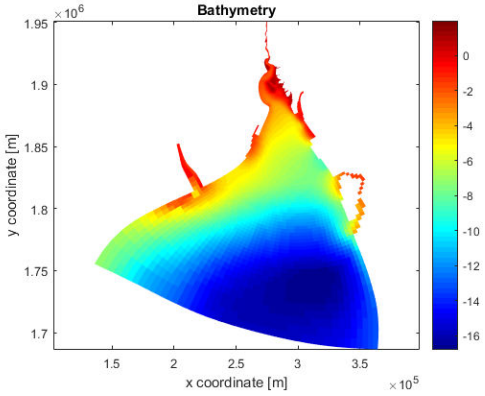

(d) Bathymetry where upper part is changed with +2 meter.

Figure B.6: Bathymetry for the sensitivity analyse for the depth.

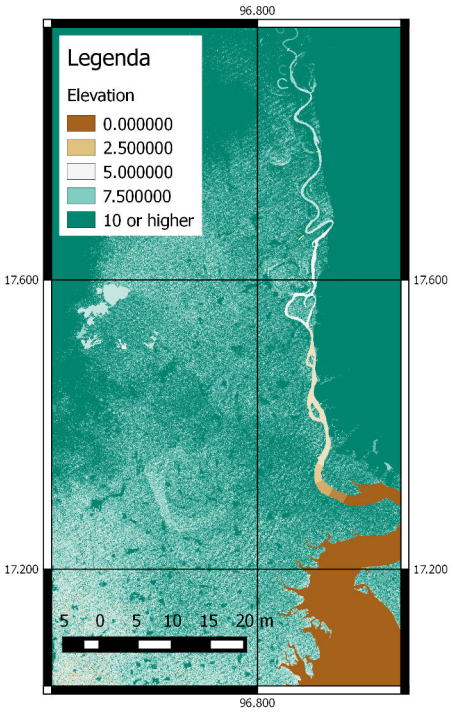

Figure B.7: SRTM map for the sittaung River

C

APPENDIX-C: BATHYMETRY CROSS-SECTIONS

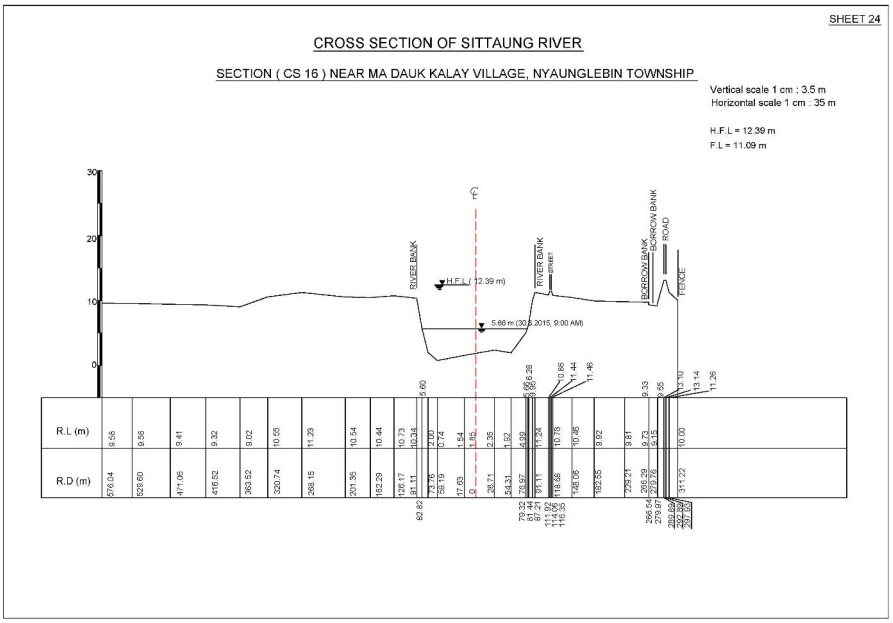

Figure C.1: Cross-section 16

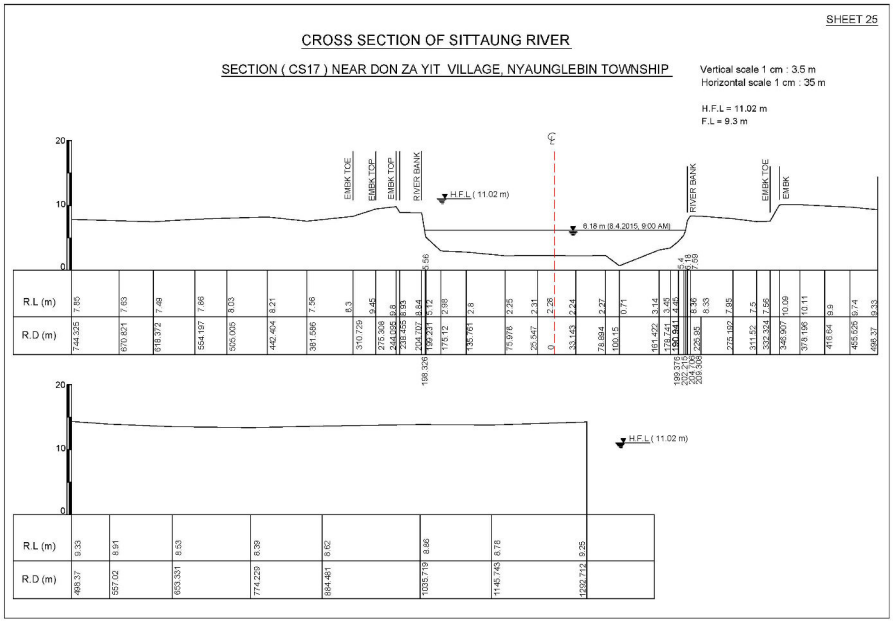

Figure C.2: Cross-section 17

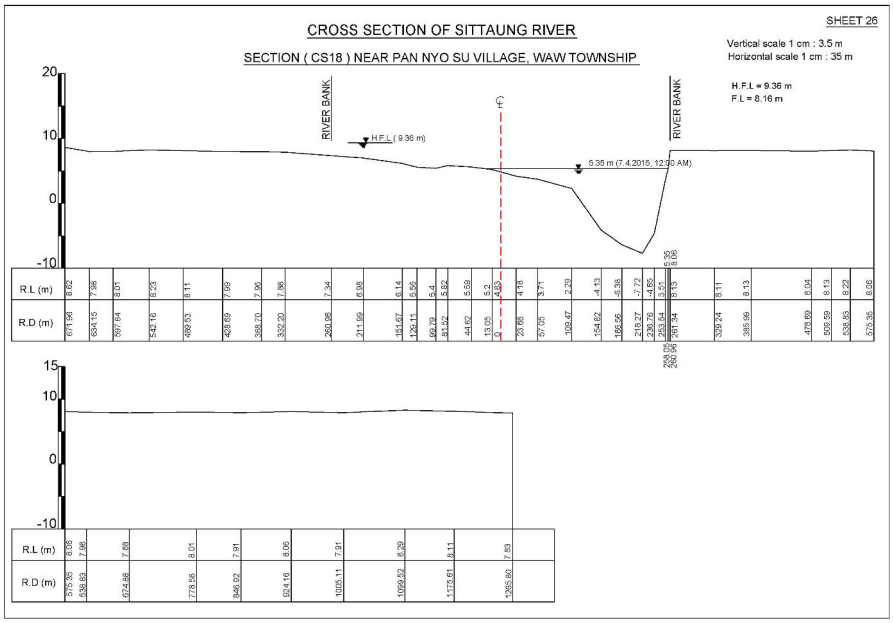

Figure C.3: Cross-section 18

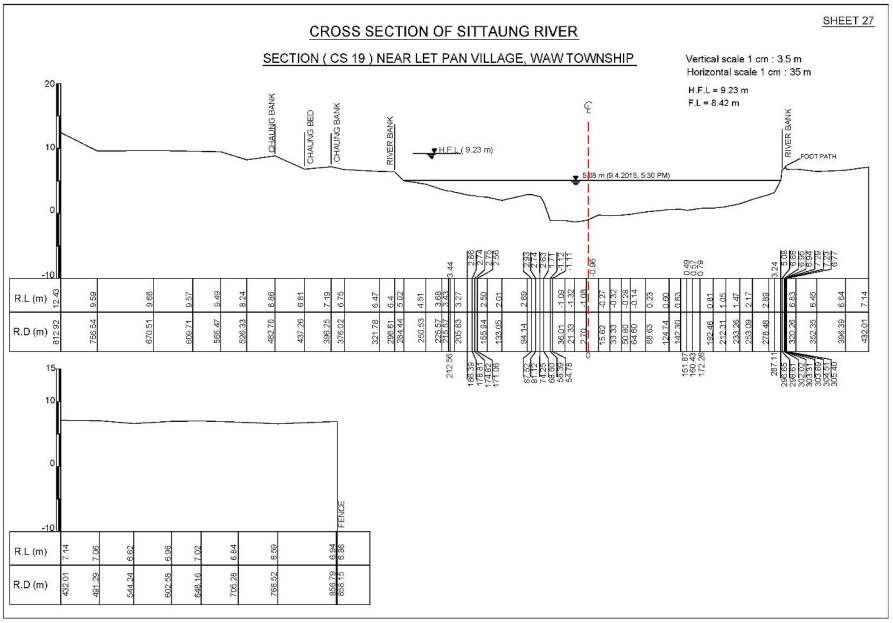

Figure C.4: Cross-section 19

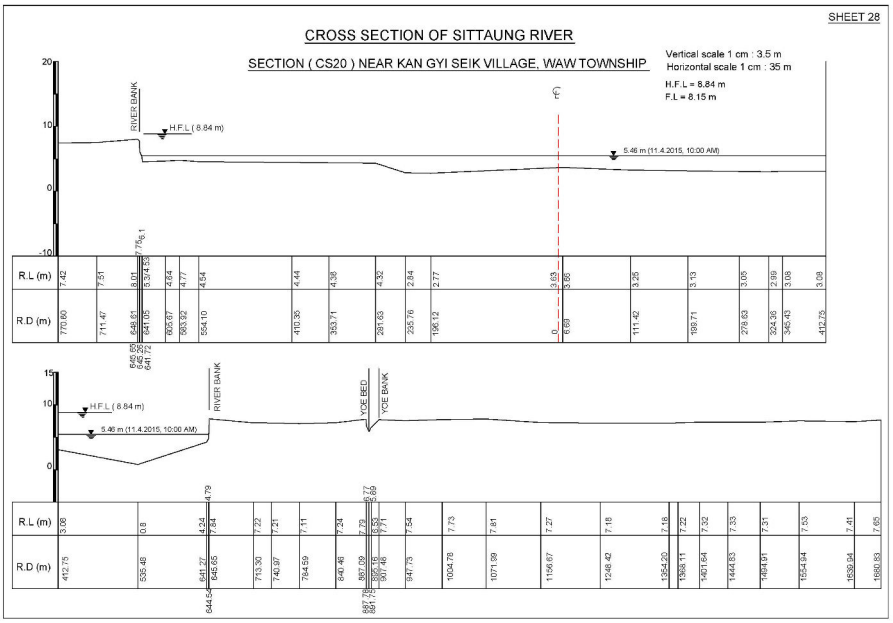

Figure C.5: Cross-section 20

BIBLIOGRAPHY

[1] H. Chanson, *Undular tidal bores: Basic theory and free-surface characteristics,* Hydraulic Engineering (2010), 10.1016/(ASCE)HY.1943-7900.0000264.

[2] S. Barthsch-Winkler and D. Lynch, *Catalof of worldwide tidal bores occurrences and characteristics,* U.S. Gov. Print. Off.[Available at http://pubs.er.usgs.gov/publication/cir1022.] (1988).

[3] H. Chanson, *Current knowlegde in tidal bores and their environemtal, ecology and cultural impacts,* Environmental fluid mechanics (2009), DOI 10.1007/s10652-009-9160-5.

[4] D. Lynch, *Tidal bores,* Scientific American (1982).

[5] M. J. Stive and J. Bosboom, *Coastal dynamics I* (2015).

[6] A. Serpy, *Tidal bores,* (2007).

[7] S. Lanzoni and G. Seminara, *On tide propagation in convergent estuaries,* AGU oceans (1998), DOI:10.1029/1998JC900015.

[8] J. P. P. Bonneton, N. Bonneton1 and B. Castelle, *idal bore dynamics in funnel-shaped estuaries,* Geophys. Res. Oceans (2015), doi:10.1002/2014JC010267.

[9] L. A. P. Bonneton, A.G. Filippini and M. Ricchiutio, *Conditions for tidal bore formation in convergent alluvial etstuaries,* Estuarine Coastal and Shelf Science (2016), DOI: 10.1016/j.ecss.2016.01.019.

[10] P. Cun-Hong and L. Hai-Yan, *2d numerical simulation of tidal bore on qiantang river using kfvs scheme,* COASTAL ENGINEERING (2010).

[11] B. L. C. Pan and X. Mao, *Tidal bore dynamics in funnel-shaped estuaries,* Hydraulic Engineering (2007), doi:10.1061/(ASCE)0733-9429.

[12] R. A. F. D. Liang, J. Xia and J. Zhang, *Study on tidal resonance in severn estuary and bristol channel,* Coastal Engineering Journal (2015), DOI: 10.1142/S0578563414500028.

[13] S. S. H. Liu, J. Li and S. Tan, *Sph modeling of tidal bore scenarios,* Natural hazzards (2010), http://dx.doi.org/10.1007/s11069-014-1374-2.

[14] G. S. Stelling and S. P. A. Duinmeijer, *A staggered conservative scheme for every froude number in rapidly varied shallow water flows,* INTERNATIONAL JOURNAL FOR NUMERICAL METHODS IN FLUIDS (2003), DOI: 10.1002/d.537.

[15] e. a. G. Donchyts, *Earth's surface water changes over the past 30 years,* Nature (2016), DOI:10.1038/nclimate311.

[16] J. F. Simpson and P. Wiles, *Reynolds stress and tke production in an estuary with a tidal bore,* Estuarine, Coastal and shelf science (2004).

[17] Y. Attema, *Delft3D model of the Ayeyarwady delta Myanmar,* Master's thesis, TUDelft (2014).

[18] E. Hendriks, *Development of a Delft3D model for the Ayeyarwady delta, Myanmar,* Master's thesis, TUDelft (2016).

[19] *Navioncs webapp,* www.navionics.com.

[20] *Sattelite radar topograpy mission,* www.earthexploder.com.

[21] *Landsat,* www.earthexploder.com (2016).

[22] *Delft3d-flow manual version 3.15,* (2011).

[23] O'Brien and M. P., *Equilibrium flow areas of tidal inlets on sandy coasts,* Waterways and harbous (1969).

[24] M. M. D'Alpaos, A.S. Lanzoni and A. Rinaldo, *On the tidal prism–channel area relations,* Jounral of Geophysical research (2010), doi:10.1029/2008JF001243.